



Contents list available at IJRED website

**International Journal of Renewable Energy Development**

Journal homepage: <https://ijred.undip.ac.id>



Research Article

# Optimal power flow solutions to power systems with wind energy using a highly effective meta-heuristic algorithm

Thi Minh Chau Le<sup>1</sup> , Xuan Chau Le<sup>2</sup>, Ngoc Nguyen Phuong Huynh<sup>3</sup>, Anh Tuan Doan<sup>3</sup>, Thanh Viet Dinh<sup>3</sup> , Minh Quan Duong<sup>3\*</sup> 

<sup>1</sup>Department of Electric Power Systems, School of Electrical and Electronic Engineering, Hanoi University of Science and Technology, Hanoi, Vietnam

<sup>2</sup>Faculty of Mechanical and Electrical, Naval Academy, Nhatrang, Vietnam

<sup>3</sup>Faculty of Electrical Engineering, The University of Danang - University of Science and Technology, Danang, Vietnam

**Abstract.** This paper implements two novel meta-heuristic algorithms, including the Coati optimization algorithm (COA) and War strategy optimization (WSO) for determining the optimal solutions to the optimal power flow problem incorporating the use of wind turbines (WTs). Two objective functions are considered in this study, including minimizing the entire electricity generation expenditure (EEGE) with the value point effect and minimizing the voltage fluctuation index (VFI). IEEE 30-bus system is chosen to conduct the whole study and validate the efficiency of the two applied methods. Furthermore, DFIG WTs are used in grids with varying power output and power factor ranges. The comparison of the results obtained from the two methods in all case studies reveals that WSO is vastly superior to COA in almost all aspects. In addition, the positive contributions of WTs to the EEGE and VFI while they are properly placed in the grid are also clarified by using WSO. As a result, WSO is acknowledged as a highly effective search method for dealing with such optimal power flow (OPF) problems considering the presence of renewable energy sources.

**Keywords:** Optimal power flow; renewable energy sources; wind turbines; Coati optimization algorithms; War strategy optimization



@ The author(s). Published by CBIORE. This is an open access article under the CC BY-SA license (<http://creativecommons.org/licenses/by-sa/4.0/>).

Received: 1<sup>st</sup> January 2023; Revised: 4<sup>th</sup> March 2023; Accepted: 14<sup>th</sup> March 2023; Available online: 30<sup>th</sup> April 2023

## 1. Introduction.

Solving the optimal power flow problem is acknowledged as the top priority for maintaining the steady state of the entire power system in operation (Gao *et al.*, 2018, Frank *et al.*, 2012). The steady state of a power system is defined by a set of variables, including the active and reactive power produced by all generators, the voltage generated by all generators, the reactive power supplied by shunt capacitors, the transformer tap settings, the voltage magnitude of all loads, and the allowed apparent power in each branch (Frank *et al.*, 2012). The values of these variables must be located within their allowable boundaries; otherwise, the steady state of a given power system cannot be established. Before solving any OPF problems, the selection of control and dependent variables will take place in advance. Generally, the control variables consist of the active power of generators (excluding the generator at the slack bus), the voltage magnitude of all generators, the reactive power supplied by all shunt capacitors, and the transformer tap settings (Frank *et al.*, 2012). While the control variables are fully determined, the calculation of the dependent variables is executed by using Matpower (Zimmerman & Murillo-Sánchez, 2016) to reach the values of the active power loss of the generator connected to the slack bus, the voltage magnitude of all load buses, the reactive power of all generators, and the apparent power in all branches. According to (Zimmerman & Murillo-Sánchez, 2016),

Matpower is supplied as independent add-in package which can be used to solve a wide range of the operational problems in power system such as: power flow (PF), continuation power flow (CPF), extensible optimal power flow (OPF), unit commitment (UC) and stochastic, secure multi-interval OPF/UC. The process of solving OPF problem can consider different objective functions such as minimizing the EEGE, minimizing the entire active power loss (EAPL), minimizing the entire emissions (EE), minimizing the voltage stability index, and so on (Gao *et al.*, 2018).

The significance of OPF problems in power system operation has attracted the attention of many researchers. Moreover, OPF is also recognized as a large-scale and non-convex problem; hence, solving the OPF problems is not an easy task. The implementation of classical methods like the Jacobian matrix or Gauss-Seidel distribution is infeasible due to their poor efficiency. On the contrary, the application of meta-heuristic algorithms is acknowledged to be a highly affordable solution. Previous studies have successfully applied meta-heuristic algorithms for reaching optimal solution of OPF problems with different objective functions. These algorithms are comprised of conventional and modified versions such as Particle swarm optimization (PSO) and its improved version (Rojanaworahiran *et al.*, 2021, Tran *et al.*, 2016), Harris hawk optimization (HHO) (Birogul 2016), Grey wolf optimization (Ladumor *et al.*, 2017), Self-learning Cuckoo search algorithm (SLCSA) (Nguyen *et al.*,

\* Corresponding author  
Email: [dmquan@dut.udn.vn](mailto:dmquan@dut.udn.vn) (M.Q.Duong)

2018), modified Jaya algorithm with the adaptive factors (MJAYA) (Warid 2020), Marine predator algorithm (MPA) (Farhat *et al.*, 2022), Gorilla troop algorithm (GTA) (Ginidi *et al.*, 2022), Ant lion optimization (ALO) (Tiwari *et al.*, 2020), Slime mould algorithm (SMA) (Khunkitti *et al.*, 2021), Social spider algorithm (SSA) (Nguyen 2019), Krill herd algorithm (KHA) (Abdollahi *et al.*, 2020), and Sine cosine optimization algorithm (SCOA) (Messaoudi *et al.*, 2020). These studies have shown different results obtained by different metaheuristic algorithms for some tests with large scale system up to 118 nodes. In addition, different single objective functions were optimized for comparisons. Basically, original algorithms could find highly feasible solutions, but the quality of the solutions are worse than those obtained by improved versions of the original algorithms. However, a sole vague problem from some of these studies is the determined allowable range of voltage as well as tap changer. Different ranges can lead to different results and the comparison can be unfair among methods. Some studies have shown the ranges and reported optimal control variables for verification but some of studies have ignored these issues. Basically, an optimal solution must satisfy all constraints before its quality is evaluated via the values of objective function. If control variables and dependent variables are not shown, the verification of solutions' validation cannot be accomplished. So, the conclusion on the performance of these algorithms without showing optimal control variables cannot be approved.

Recently, the trend of incorporating renewable energy sources (RESs) such as wind and solar energies in the power system has become more popular due to the rise of environmental problems and the depletion of fossil fuels. To follow the current trend, many research about OPF problems incorporating RESs are being conducted. Besides, meta-heuristic algorithms are mostly used as a highly effective searching method. The implementation of meta-heuristic algorithms to solve the OPF problem incorporating renewable energy is more popular, such as Artificial Bee Colony (ABC) (Ahgajan *et al.*, 2021), Equilibrium Optimizer Algorithm (EOA) (Nusair *et al.*, 2021), Jaya Algorithm (JAYA), and its variants, including Modified Jaya Algorithm (MJY) and the hybrid of Firefly and Jaya algorithm (Warid *et al.*, 2016; Elattar, *et al.*, 2019; and Alghamdi 2021), Multi-objective Coronavirus Herd Immunity Algorithm (MOCOHIA) (Ali 2021), Non-dominated sort grey wolf optimizer (NDGWO), Modified Rao algorithm (MRAO) (Hassan *et al.*, 2021), Effective cuckoo search algorithm (ECSA) (Pham *et al.*, 2022), Barnacle mating optimizer (BMO) (Sulaiman *et al.*, 2021), Manta ray foraging optimization (MRFO) (Alasali *et al.*, 2021), Differential evolution (DE) (Duman *et al.*, 2020), Enhanced genetic algorithm (GA) (Reddy, 2016), Flower pollination algorithm (FPA) (Abdullah *et al.*, 2019), White shark algorithm (WSA) (Ali *et al.*, 2022) and Crow search algorithm (CRSA) (Bamane 2019), Modified Equilibrium algorithm (MEA) (Duong *et al.*, 2021), and Modified coyote optimization algorithm (Li *et al.*, 2019) (MCOA). These algorithms were applied for three four cases with the placement of only WTs (Ahgajan *et al.*, 2021, (Warid *et al.*, 2016, Elattar, *et al.*, 2019), the placement of only solar photovoltaic arrays (Pham *et al.*, 2022; Duong *et al.*, 2021), both WTs and solar photovoltaic arrays (Nusair *et al.*, 2021; Alghamdi 2021 - Hassan *et al.*, 2021; Sulaiman *et al.*, 2021 - Bamane 2019). Some studies have fixed the location, but optimized size of renewable energy based distributed generators at given nodes, whereas some studies have optimized both location and size. In addition, other ideas have optimized three parameters, including location, size, and the number of units. The more parameters are optimized, the more complicated the studies are. In general, all studies have sufficient contribution to transmission networks as considering renewable energies. However, some aspects have been ignored in the studies. The

studies have not considered thermal unit valve effects, different rates of power ranges, and the impact of determined placement location on the systems.

In this study, we applied two meta-heuristic algorithms, including the Coati optimization algorithm (COA) (Dehghani *et al.*, 2022) and the War strategy optimization (WSO) (Ayyarao *et al.*, 2022) to solve the OPF problem while incorporating the presence of wind energy. We considered the wind power plants as generators, which can produce both active power and reactive power. The study uses an IEEE 30-bus transmission system to evaluate the efficiency of the two applied algorithms with two objective functions, including minimizing EEGE and minimizing the voltage fluctuation index (VFI). In addition, two different locations are adopted to install WT for each case to achieve the optimal value of the considered objective functions. Two different nodes 3 and 30 are in turn selected to place one WT and two cases of rated power, 10 MW and 30 MW are tried for investigating the cost reduction and the voltage improvement. About the applied methods, COA is developed by imitating the living practices of coatis in nature, while WSO is proposed based on simulating the moving strategy of army groups on the battlefield. COA and WSO were both proposed in mid- and early 2022. As reported in the studies (Dehghani *et al.*, 2022; Ayyarao *et al.*, 2022), the algorithms provide surprising performance over many previous algorithms throughout various benchmarks. The primary contributions of the whole study can be briefly listed as follows:

- Successfully apply two novel meta-heuristic algorithms, including Coati optimization algorithm (COA) and War strategy optimization (WSO) to solve the OPF problem in which the presence of WTs is evaluated.
- Clarify the positive effects in both economic and technical aspects while WTs are installed properly in the transmission system.

## 2. Problem formulation

### 2.1. The main objective functions

The paper shows the effectiveness of the placement of renewable energies in power systems with a high power from conventional power plants. The first effectiveness shows the cost reduction for the power plants meanwhile the second effectiveness proves the improvement of voltage thanks to the reduction of current on transmission lines. To indicate the results, two single objective functions are established and optimized. The detail of them is as follows.

#### 2.1.1. Minimization of entire electricity generation expenditure (EEGE)

The first single objective function in this paper focuses on minimizing the EEGE of thermal power plants in the power system with the additional generation of renewable energies-based generators. EEGE is determined by the expenditure of fossil fuels such as oil, coal, gas, etc. to run the thermal power plants. While all types of the fossil fuels are getting higher price due to the overuse, the EEGE of thermal power plants must be minimized as large as possible. According to (Khunkitti *et al.*, 2021), the EEGE is modelled as Equation (1):

$$\text{Minimize } EEGE = \sum_{g=1}^{N_g} \tau_g + \varphi_g P G_g + \omega_n (P G_g)^2 \quad (1)$$

Where,  $EEGE$  is the entire electricity generation expenditure,  $P G_g$  is the active power generated by thermal power plant  $g$ ,  $N_g$

is the number of existing thermal power plant in grid,  $\tau_g$ ,  $\varphi_g$ , and  $\omega_n$  are the fuel utilizing factor of thermal power plant  $g$ . As considering valve effects from thermal units, the objective is rewritten as Equation (2):

$$\text{Minimize } EEGE = \sum_{g=1}^{N_G} \tau_g + \varphi_g PG_g + \omega_n (PG_g)^2 + \left| \sigma_g \times \sin \left( \varepsilon_i \times (PG^{min} - PG_g) \right) \right| \quad (2)$$

Where  $\sigma_g$  and  $\varepsilon_i$  are the given coefficients, and  $PG^{min}$  is the lowest active power produced by thermal power plant.

### 2.1.2. Minimization of voltage fluctuation index (VFI)

The second objective function is about the quality of the load voltage. Basically, the voltage of loads is possible to vary from a smaller value than 1.0 Pu to a higher value than 1.0 Pu as long as the voltage is still within an operating range. However, if the voltages fluctuate in a big range, loads cannot be working stably and effectively. So, voltage quality much be supervised via the value of VFI. As the index is zero or very close to zero, the loads are stable. On the contrary, if the index moves far away from zero, the load cannot reach its normal operation status. The expression is mathematically presented in Equation (3):

$$\text{Minimize } VFI = \sum_{d=1}^{N_D} |U_d - 1| \quad (3)$$

Where, VEF is the voltage fluctuation index,  $N_D$  is the number of load bus,  $U_d$  is the voltage magnitude at load bus  $d$ .

## 2.2. The involved constraints

### 2.2.1. The working constraints of thermal generators

This constraint regards the legal boundaries of three parameters, including the active, reactive power produced by thermal generators and their generation voltages. The parameters must satisfy the formulas (4), (5) and (6) below:

$$PG^{min} \leq PG_g \leq PG^{max} \quad (4)$$

$$QG^{min} \leq QG_g \leq QG^{max} \quad (5)$$

$$VG^{min} \leq VG_g \leq VG^{max} \quad (6)$$

Where,  $PG^{min}$  and  $PG^{max}$  are the lowest and the highest active power produced by thermal power plant  $g$ ,  $QG^{min}$  and  $QG^{max}$  are the lowest and the highest reactive power output produced by thermal power plant  $g$ ,  $VG^{min}$  and  $VG^{max}$  are the lowest and highest generation voltages generated by thermal power plant  $g$ ,  $PG_g$ ,  $QG_g$  and  $VG_g$  are operating values of active power, reactive power and generation voltage of the  $g$ th generator.

### 2.2.2. The equal constraints

This constraint means that, the entire active and reactive power produced by all existing generating sources in the power system must be the same as the entire active and reactive power required by all loads together with line loss. The constraints are shown in Equation (7) and (8) below:

$$\sum_{g=1}^{N_G} PG_g + \sum_{w=1}^{N_W} PWT_w + PLS - PLD = 0 \quad (7)$$

$$\sum_{g=1}^{N_G} QG_g + \sum_{s=1}^{N_S} QS_s + \sum_{w=1}^{N_W} QWT_w + QLS - QLD = 0 \quad (8)$$

With

$$QS^{min} \leq QS_s \leq QS^{max} \text{ with } s = 1, \dots, N_S \quad (9)$$

$$PWT^{min} \leq PWT_w \leq PWT^{max} \text{ with } w = 1, \dots, N_W \quad (10)$$

$$QWT^{min} \leq QWT_w \leq QWT^{max} \text{ with } w = 1, \dots, N_W \quad (11)$$

In the Equations (7-11),  $PWT_w$  and  $QWT_w$  are the active and reactive power supplied by WT  $w$ .  $N_W$  is the number of WTs in grid.  $PWT^{min}$  and  $PWT^{max}$  are the lowest and the highest active power supplied by WT.  $QWT^{min}$  and  $QWT^{max}$  are the lowest and the highest reactive power supplied by WT. Note that, the value of  $QWT_w$  is determined based on  $PWT_w$  and power factor ( $PF_w$ ) of WT $w$ .  $PLS$  and  $QLS$  are the active and reactive power loss on all transmission lines.  $PLD$  and  $QLD$  are active and reactive power required by all loads.  $QS^{min}$  and  $QS^{max}$  are the lowest and the highest reactive power supplied by the  $s^{th}$  shunt capacitor.  $QS_s$  is the reactive power supplied by shunt capacitor  $s$  and  $N_s$  is the number of shunt capacitors in grid.

Note that the WTs used in this study utilize DFIG technology, and therefore they can inject both active and reactive power to the grid.

### 2.2.3. The security constraints

This constraint is mainly related to the legal limits of load voltages and the maximum limit of the apparent power allowed to run through distribution lines. Power flow solutions should have load voltage and line power within allowable bounds as Equations (12)-(14):

$$VD^{min} \leq VD_d \leq VD^{max} \text{ with } d = 1, \dots, N_D \quad (12)$$

$$SBr_r \leq SBr_r^{max} \text{ with } r = 1, \dots, N_R \quad (13)$$

$$TL^{min} \leq TL_t \leq TL^{max} \text{ with } t = 1, \dots, N_T \quad (14)$$

Where,  $VD^{min}$  and  $VD^{max}$  are the lowest and the highest voltage magnitude of all loads,  $VD_d$  is the voltage of load  $d$ ,  $N_D$  is the number of loads in the system,  $SBr_r$  is the apparent power of the transmission line  $r$ ,  $N_R$  is number of transmission lines of the system,  $SBr_r^{max}$  is the maximum apparent power that the transmission line  $r$  can work stably.  $TL_t$  is the tap setting of the transformer  $t$ ,  $N_T$  is the number of transformers in the grid,  $TL^{min}$  and  $TL^{max}$  are the lowest and the highest location of the transformer tap setting.

## 3. The computing methods

As mentioned earlier, this study applied two novel meta-heuristic algorithms for solving the OPF problems, including COA and WSO. The important difference between the two applied methods is their update methods for new solutions which is briefly presented in the next subsections:

### 3.1. The Coati optimization algorithm

The coati optimization algorithm (COA) is established by simulating the hunting behavior of coatis in nature. There are two main behaviors, including attacking and hunting the prey and escaping from the enemies. These behaviors are also the foundation of the two phases in the update process for new solutions to the algorithm. The mathematical expressions of each phase will be briefly described as Equations (15)-(17) (Dehghani et al., 2022):

- Phase 1:

$$C_j^{new1} = C_j + \gamma \times (IG - IR \times C_j), \text{ with } j = 1, 2, \dots, \frac{PN}{2} \quad (15)$$

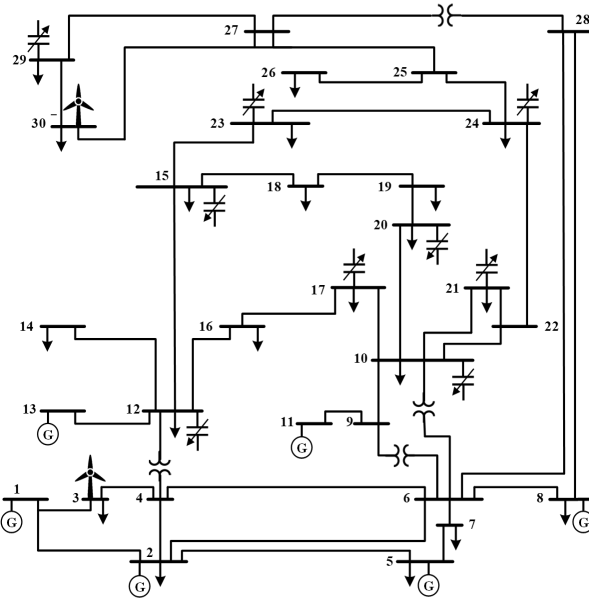


**Fig 1.** The modified configuration of IEEE 30-bus transmission system with WTs at bus 3 and bus 30

Then,

$$C_j^{new1} = \begin{cases} C_j + \gamma \times (IG - IR \times C_j), & \text{if } F_{IG} < F_{C_i} \\ C_j + \gamma \times (C_j - IG), & \text{otherwise} \end{cases} \quad (16)$$

and  $j = \frac{PN}{2} + 1, \frac{PN}{2} + 2, \dots, PN$

In the Equations (15-16),  $C_j^{new1}$  is the location of Coati  $j$  among the population,  $\gamma$  is the random value in the interval of 0 and 1,  $IG$  is the prey location,  $IR$  is the random value between 1 and 2,  $PN$  is the population number.

- Phase 2:

$$C_j^{new2} = C_j + (1 - 2\gamma) \times (LB_j + \gamma \times (LB_j - HB_j)), \text{ with } j = 1, 2, \dots, PN \quad (17)$$

Where  $LB_j$  and  $HB_j$  are the lowest and the highest boundary of the search space.

### 3.2. The War strategy optimization.

The war strategy optimization (WSO) is proposed based on the movements of the army troops in a war following two strategies, which are attacking and defending. The switching appropriately between these two strategies plays the key role for modelling the update mechanism of the algorithm. The update for new solutions of WSO is executed by using Equation (18) (Ayyarao et al., 2022):

$$W_i^{new} = \begin{cases} W_i + 2 * \pi * (CD - KG) + rn * (we_i * KG - W_i), \\ W_i + 2 * \pi * (KG - W_{rn}) + rn * (we_i * CD - W_i), \end{cases} \quad (18)$$

In the equation above,  $W_i^{new}$  is the new location of soldier  $i$  at the next iteration;  $\pi$  and  $rn$  are the values randomly generated in the interval of 0 and 1.  $CD$  and  $KG$  are the location of the general and the kings in the search space.  $we_i$  is the scale index of the soldier  $i$ ,  $W_{rn}$  is the random soldier randomly selected from the initial population, and  $RF$  is the reference factor.

## 4. Numerical results and discussion

In this part, COA and WSO are implemented to find the optimal solution to OPF problems considering the presence of WTs in different case studies. The IEEE-30 transmission power system was selected to conduct the study. The basic structure of the system consists of 6 thermal power plants (located at buses 1, 2, 5, 8, 11 and 13), 4 transformers, 41 transmission lines, 24 load buses, and 9 shunt capacitors. The system is illustrated in Figure 1 and the whole data of the grid are taken from (Nguyen 2019). As mentioned earlier, the study aimed to minimum values of the two separated objective functions, including EEEG and VFI. Data of thermal units are taken from (Nguyen 2019). According to (Warid et al., 2016; Elattar & ElSayed, 2019), the authors have proven that buses 3 and 30 are, respectively, the worst and best locations for placing WTs to achieve the objective functions, including the ones considered in this study. Therefore, in this study, we also placed WTs at the same locations to investigate the real performance of the two applied methods and impact of WTs on fuel cost and voltage profile. Each added wind turbine is supposed to have the power factor from 0.8 to 1.0 and the maximum generation of either 10 or 30 MW. Four study cases are simulated, and one wind turbine is separately placed at two different nodes, node 3 and node 30 for each study case. The objective function result from each node is compared for evaluation. The descriptions of the four study cases are summarized as follows:

- Case 1: Place one wind turbine with the maximum generation of 10 MW for EEEG reduction.
- Case 2: Place one wind turbine with the maximum generation of 30 MW for EEEG reduction.
- Case 3: Place one wind turbine with the maximum generation of 10 MW for VFI minimization.
- Case 4: Place one wind turbine with the maximum generation of 30 MW for VFI minimization.

The initial parameters of the two applied methods in terms of population, maximum number of iterations, and number of independent runs are fairly set at 20, 50, and 50, respectively. Simulations are executed on a personal computer Core i7, 2.39 GHz and 8 GB of RAM, and MALAB program version 2018a.

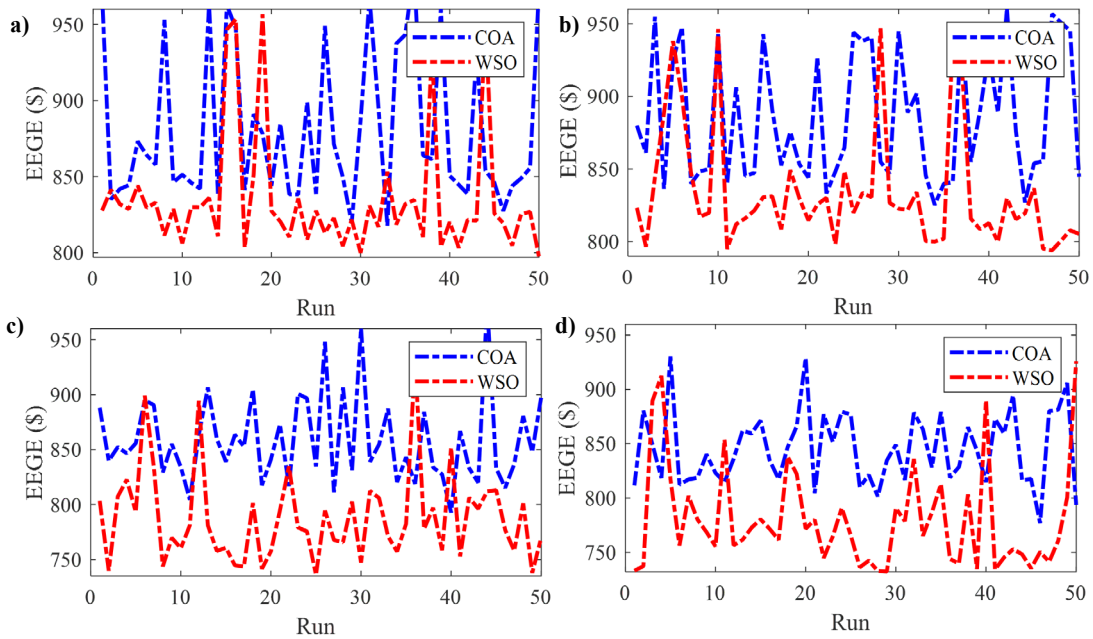


**Fig 2.** The results achieved after 50 independent runs: (a) Case 1 with WT at node 3; (b) Case 1 with WT at node 30; (c) Case 2 with WT at node 3; (d) Case 2 with WT at node 30

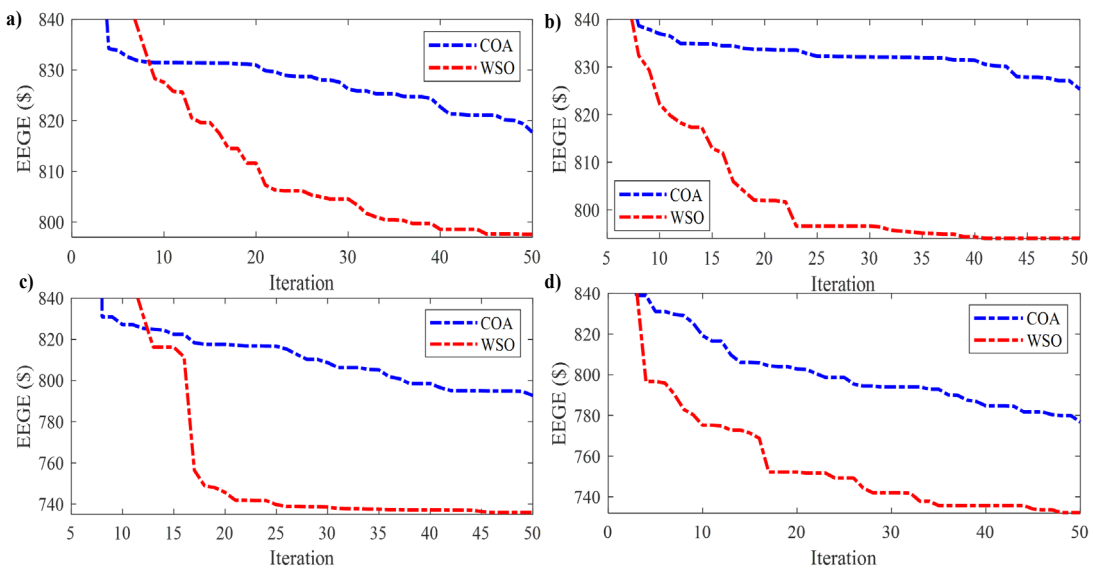


**Fig 3.** The best convergences obtained by COA and WSO: (a) Case 1 with WT at node 3; (b) Case 1 with WT at node 30; (c) Case 2 with WT at node 3; (d) Case 2 with WT at node 30

4.1. The results achieved for Case 1 and Case 2.

Figure 2 presents the EEGE values obtained by both COA and WSO for Case 1 and Case 2 after 50 independent runs. The figure of all runs can be a good evidence for evaluating the effectiveness and stability of algorithms (Duong *et al.*, 2021). Subfigures a) and b) describe the results obtained by the two applied methods for Case 1 with turbine at node 3 and node 30, respectively. Subfigures c) and d) show the similar value obtained for Case 2 with turbine at node 3 and node 30. In these subfigures, the blue line shows the values obtained by COA, and the red line illustrates the results achieved by WSO. The observation from Figure 2 indicates that WSO can reach much more optimal values than COA throughout 50 independent runs.

The best convergences achieved by COA and WSO among 50 independent runs are depicted in Figure 3. Similar to Figure 2, the results of Case 1 are shown in Subfigures a) and b),

while the results of Case 2 are reported in Subfigures c) and d). WSO always reaches the optimal values of EEGE much faster than COA in all subfigures. WSO only requires over 45 iterations for reaching the optimal value in the case WTs placed at bus 3 with different rated powers, including 10MW and 30MW, as shown in Subfigures 3a and 3c, whereas COA cannot perform the same even when the last iteration is done. The observation from Subfigures 3b and 3d also points out the outstanding performance of WSO over COA. In these subfigures, WSO requires over 40 and 45 iterations to reach the optimal results for the Case WT placed at bus 30 with different rated power, including 10MW and 30MW, while COA again cannot get the same optimal value. This means that WSO is both a powerful and highly efficient search method. On the contrary, COA shows its poor efficiency for both Case 1 and Case 2 because the method cannot reach any optimal values of EEGG.

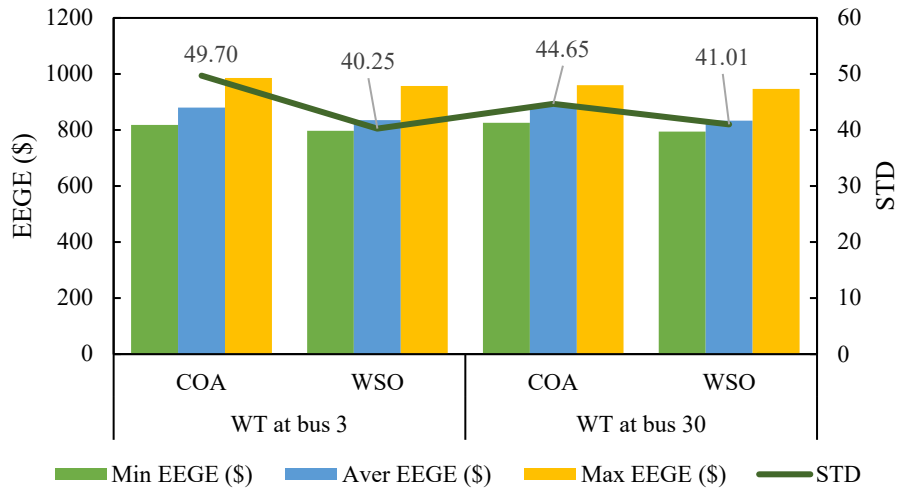


Figure 4. The comparison between the COA and WSO in different aspects of Case 1

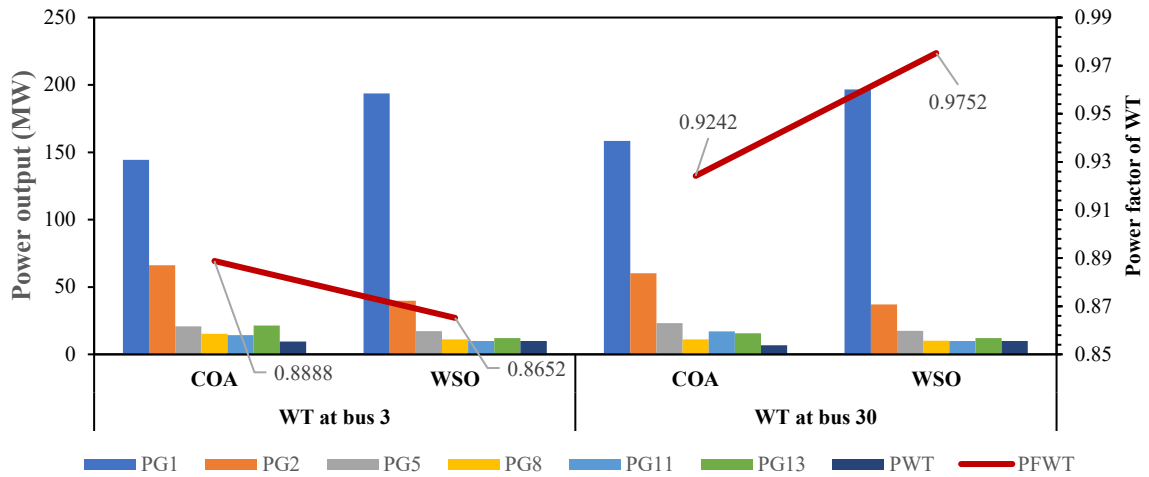


Fig 5. Power output of each thermal generators achieved by COA and WSO in Case 1

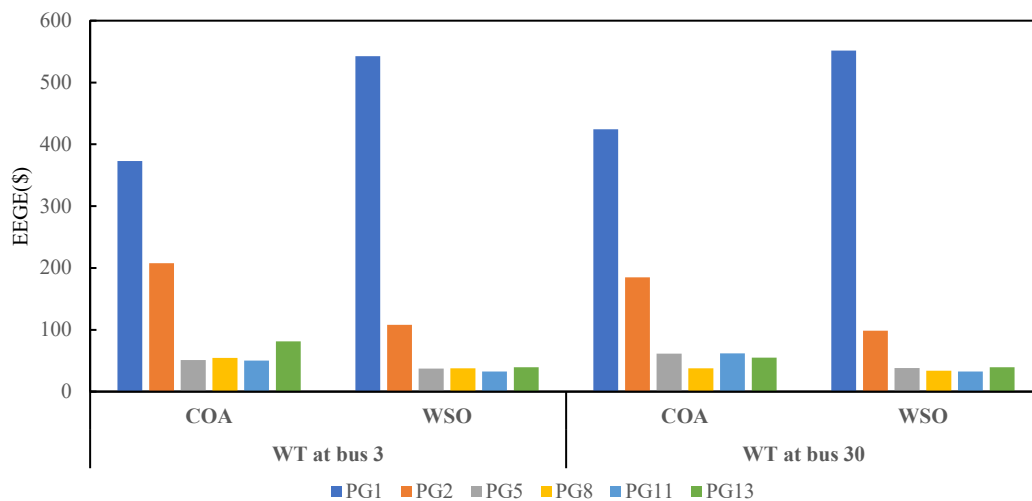


Fig 6. The EEGE values of each thermal generator achieved by COA and WSO in Case 1

The comparison between COA and WSO on different aspects of Case 1 is presented in Figure 4. In the figure, the minimum EEGE (Min EEGE), average EEGE (Aver EEGE), maximum EEGE (Max EEGE), and standard deviation (STD) achieved by the two applied methods are evaluated. The results reveal that WSO completely outperforms COA in all considered

aspects. Specifically, for the case that WT is placed at node 3, the results achieved by the WSO in each comparison criterion are, respectively, \$797.5613 for the minimum EEGE, \$834.8322 for the mean EEGE, \$956.7061 for the maximum EEGE, and 40.2482 for the standard deviation, while the similar values obtained by COA are, respectively, \$817.7237, \$880.2532,

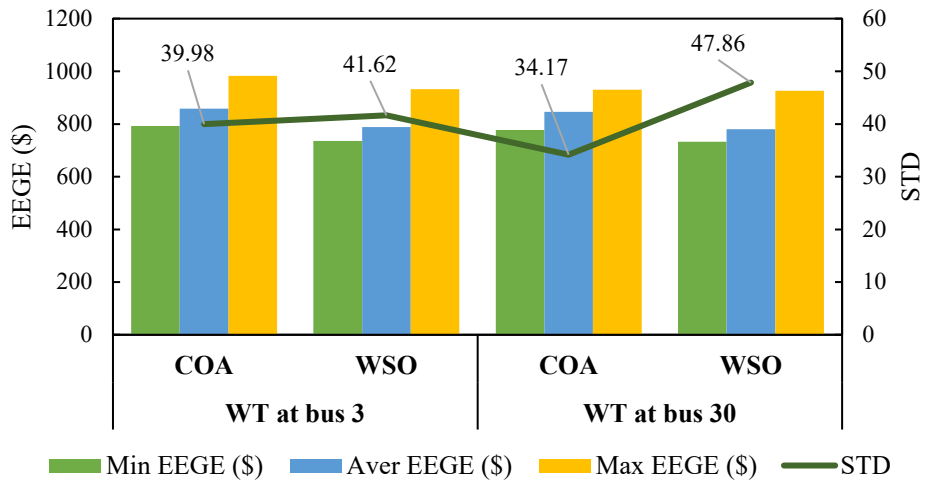


Fig 7. The comparison between COA and WSO in different aspects of Case 2

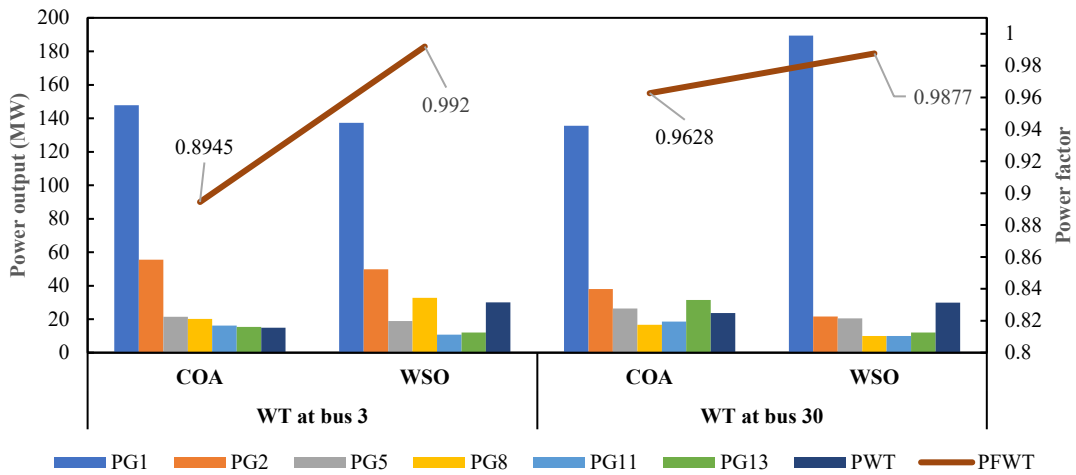


Fig 8. Power output of each thermal generators achieved by COA and WSO in Case 2

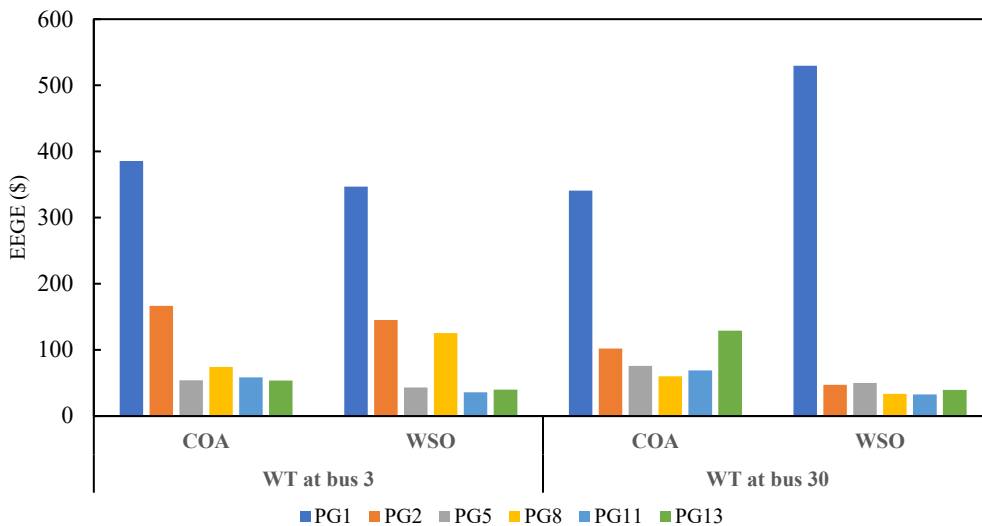


Fig 9. The EEGE values of each thermal generator achieved by COA and WSO in Case 2

\$985.648, and 49.7034. The saving costs of WOA over COA for this circumstance on the first three criteria are \$20.1624, \$45.421, and \$28.9419, corresponding to 2.47%, 5.16%, and 2.93%. On the other hand, in the case that WT is placed at node 30, the results reached by WOA on the four comparison criteria are \$794.0225, \$833.3581, \$946.8835, and 41.0088, while those of COA are \$825.3336, \$884.9905, \$960.1789, and 44.6468. By

doing some simple calculations, the saving costs of WOA compared with COA in this circumstance on the first three criteria are \$31.3081, \$51.6054, and \$13.2954 corresponding with 3.79%, 5.83% and 1.38%. Clearly, WOA is much more effective than COA in terms of all costs. In Figure 5, the active power supplied by six thermal generators (represented by PG1, PG2, PG5, PG8, PG11, and PG13 for generators at bus 1, 2, 5, 8,

11 and 13) achieved by COA and WSO in Case 1 are shown. Besides, the active power injected by the WT and its power factor are also given. Figure 6 describes the EEGE belonging to each thermal generator in Case 1. Figure 7 shows the contrast of the EEGE values obtained in Case 2 by COA and WSO through different criteria, including Min EEGE, Aver EEGE, Max EEGE, and STD. WSO shows its superiority to COA in the first three criteria by always reaching the lower values. Clearly, WSO provides better efficiency for determining the optimal value while dealing with the considered problem. Similar to Case 1, the results obtained by the two applied methods in this case are also compared based on four criteria as mentioned earlier. Particularly, for the case WT is placed at node 3, the results obtained by WSO on the first three criteria are, respectively, \$735.9254, \$788.0952, and \$932.0582, while those of COA are \$792.7494, \$858.6724, and \$982.994. It is easy to figure out that WSO always saves a particular value of EEGE on each comparison criterion over COA. Specifically, the saving costs on the first three criteria of WSO over COA are \$56.824, \$70.58, and \$50.94. These saving costs correspond to a percentage of 7.16%, 8.22%, and 5.18%. Next, for the case with WT placed at node 30, the superiority of WSO is continuously maintained over COA. Particularly, the results achieved by WSO on Min EEGE, Aver EEGE, and Max EEGE are, respectively, \$732.2329, \$780.1877, and \$926.1401, while similar values resulted by COA are, \$776.8398, \$845.6318, and \$930.326. Apparently, WSO can save \$44.61, \$65.44, and \$4.19, respectively. These saving costs are equal to 5.74%, 7.74%, and 4.18% for each criterion. In terms of STD, COA can reach a lower value than WSO in both cases. The power supplied by thermal generators, the active power generated by WTs, and their power factors achieved by the two applied methods in Case 2 are reported in Figure 8. Next, the EEGE value of each thermal generator is described in Figure 9.

4.2. The results achieved in Case 3 and Case 4.

In this section, the efficiency of both COA and WSO is investigated with the objective function of minimizing VFI. The investigation is conducted through two scenarios, including placing WTs at buses 3 and 30, independently. Besides, the positive effect brought by WTs is also given.

Table 1 shows the VFI values obtained by both COA and WSO for Case 3. Besides, VFI values in the base case without WTs obtained by the two applied methods are also given. The results reached by COA do not show any improvement in VFI while WTs are placed on the grid. Particularly, for the base case without WT, the VFI achieved by COA is only 0.1193, whereas with WT placed at bus 3 and bus 30, the VFI values for the cases are 0.1240 and 0.1558, respectively. In contrast, the results achieved by WSO point out a huge improvement in the VFI value when the WT is properly placed at bus 30. The VFI in this case is only 0.09514, whereas the comparable value resulting from the base case is 0.1160. By converting into percentage, the application of WSO for the WT placed at bus 30 is more effective than the base case up to 21,93%. Besides, the results obtained by WSO for the case WT placed at bus 3 also indicates the improvement on VFI value, but the effectiveness is not as much as placing WT at bus 30 and is only 0.91%.

Table 2 presents the VFI values reached by COA and WSO in Case 4. The observation in the table indicates the same phenomenon as in Case 3. That is, while WTs are installed in the grid, COA maintains its low efficiency and does not improve VFI values. Specifically, for the cases with WTs placed at bus 3 and bus 30, the VFI values obtained by COA are 0.1658 and 0.1890, while the similar value given by COA in the Base case is only 0.1193. On the contrary, WSO still proves itself to be an effective method by achieving a clear improvement in VFI value while the

**Table 1**  
The results comparison between COA and WSO on different aspects in Case 3

Result	BASE COA	COA with WT at bus 3	COA with WT at bus 30	BASE WSO	WSO with WT at bus 3	WSO with WT at bus 30
Min VFI	0.1193	0.1240	0.1558	0.1160	0.11495	0.09514
Aver VFI	0.2777	0.3486	0.3107	0.1902	0.1664	0.1511
Max VFI	0.6610	0.6958	0.6979	0.4081	0.2900	0.3680
STD	0.1449	0.1401	0.1270	0.0654	0.0346	0.0389



**Fig 10.** Voltage values at buses achieved by WSO: a) Place WT at bus 3; b) Place WT at bus 30



**Table 2**  
The results comparison between COA and WSO on different aspects in Case 4

Result	BASE COA	COA with WT at bus 3	COA with WT at bus 30	BASE WSO	WSO with WT at bus 3	WSO with WT at bus 30
Min VFI	0.1193	0.1658	0.1890	0.1160	0.1115	0.1022
Aver VFI	0.2777	0.1902	0.4405	0.1902	0.2225	0.2067
Max VFI	0.6610	0.4081	1.0334	0.4081	0.9628	0.5518
STD	0.1449	0.0654	0.1912	0.0654	0.1498	0.1031



**Fig 11.** The voltage profile at all buses obtained by COA and WSO in Case 3 and Case 4

WT is optimally placed at bus 30. Particularly, for the case WT placed at bus 30, the VFI is only 0.1022 corresponding to the improvement of 13.50 % over the Base case. The observation from the case WT placed at bus 3 also shows the enhancement on VFI compared with the Base case but the percentage in the case is only 4.036%.

The observation on the results given by both Case 3 and Case 4 indicates that the placement of a WT 30 MW in Case 4 dose not result the same percentage of the improvement on VFI value. Due to the use of DFIG technology, a WT can inject both active and reactive power into grid, that means that, the more active power is pumped into grid, the more reactive power is. The increment of reactive power value at buses near by the WT's position accidentally increases the voltage value at these buses.

Therefore, the VFI in the case with larger rated power of WT results in a smaller effectiveness than the case with smaller rated power of WT.

In Figure 10, the voltage at all buses obtained by WSO is presented in three scenarios, including without a WT, with a WT at bus 3, and with a WT at bus 30. In subfigure 10a, there are two different rated powers of WT's, including 10 MW and 30 MW for the scenarios for a WT placed at bus 3. The same behavior is also applied while a WT is placed at bus 30, and the results are shown in subfigure 10b. The observation in both subfigures 10a and 10b indicates that the placement of the WT at bus 30 in both scenarios shows a better improvement in VFI than when the WT is placed at bus 3.

Figure 11 provides the graphical results of the voltage profile achieved by COA and WSO in three scenarios, including 1) without WT, 2) with WT placed at bus 3, and 3) with WT placed at bus 30. In addition, subfigures a and b displayed the results of Case 3, while subfigures c and d presented the results of Case 4. The observations from all subfigures indicate that the placement of the WT at bus 30 always results in a better VFI than bus 3, regardless of whether the rated power is 10 MW or 30 MW.

## 5. Conclusions.

In this study, the Coati optimization algorithm (COA) and War strategy optimization (WSO) were successfully applied to solve the optimal power flow problem incorporating the presence of WTs in the IEEE 30-bus transmission system. The applied methods are modern meta-heuristic algorithms proposed in 2022. In the whole study, two main objective functions were considered: minimizing the entire electricity generation cost and minimizing the voltage fluctuation index. In addition, DFIG WTs were also placed into a power grid while determining the optimal solutions to the considered problem. The placement of WT into grid was devised into different cases with various specifications of WT. The results achieved by both COA and WSO were evaluated through different aspects for assessing their real efficiency. The evaluation revealed that WSO outperformed COA in almost all comparison criteria. With these witnesses, WSO was proved to be an effective and powerful search method to deal with OPF problems incorporating the presence of WTs.

However, the study has not considered uncertainty characteristic of wind speed as well as the change of load over 24 hours for one day in a year or all days of a year. In addition, OPF problem should be scaled up by integrating both wind and solar energy into a larger configuration of power system such as, IEEE-57 bus, an IEEE-118 bus, or a real power system. These neglected aspects are the limitations of the study that should be improved in future work.

## Acknowledgement

This research was funded by the Ministry of Education and Training under project number CT 2022.07.DNA.06.

## References

- Abdollahi, A., Ghadimi, A. A., Miveh, M. R., Mohammadi, F., & Jurado, F. (2020). Optimal power flow incorporating FACTS devices and stochastic wind power generation using krill herd algorithm. *Electronics*, 9(6), 1043; <https://doi.org/10.3390/electronics9061043>
- Abdullah, M., Javaid, N., Khan, I. U., Khan, Z. A., Chand, A., & Ahmad, N. (2019, March). Optimal power flow with uncertain renewable energy sources using flower pollination algorithm. In *International Conference on Advanced Information Networking and Applications* (pp. 95-107). Springer, Cham; [https://doi.org/10.1007/978-3-030-15032-7\\_8](https://doi.org/10.1007/978-3-030-15032-7_8)
- Ahgajan, V. H., Rashid, Y. G., & Tuaimah, F. M. (2021). Artificial bee colony algorithm applied to optimal power flow solution incorporating stochastic wind power. *International Journal of Power Electronics and Drive Systems (IJPEDS)*, 12(3), 1890-1899; <https://doi.org/10.11591/ijpeds.v12.i3.pp1890-1899>
- Alasali, F., Nusair, K., Obeidat, A. M., Foudeh, H., & Holderbaum, W. (2021). An analysis of optimal power flow strategies for a power network incorporating stochastic renewable energy resources. *International Transactions on Electrical Energy Systems*, 31(11), e13060; <https://doi.org/10.1002/2050-7038.13060>
- Alghamdi, A. S. (2022). A Hybrid Firefly-JAYA Algorithm for the Optimal Power Flow Problem Considering Wind and Solar Power Generations. *Applied Sciences*, 12(14), 7193. <https://doi.org/10.3390/app12147193>
- Ali, M. A., Kamel, S., Hassan, M. H., Ahmed, E. M., & Alanazi, M. (2022). Optimal Power Flow Solution of Power Systems with Renewable Energy Sources Using White Sharks Algorithm. *Sustainability*, 14(10), 6049; <https://doi.org/10.3390/su14106049>
- Ali, Z. M., Aleem, S. H. A., Omar, A. I., & Mahmoud, B. S. (2022). Economical-environmental-technical operation of power networks with high penetration of renewable energy systems using multi-objective coronavirus herd immunity algorithm. *Mathematics*, 10(7), 1201; <https://doi.org/10.3390/math10071201>
- Ayyarao, T. S., Rama Krishna, N. S. S., Elavarasan, R. M., Polumhanthi, N., Rambabu, M., Saini, G., ... & Alatas, B. (2022). War strategy optimization algorithm: a new effective metaheuristic algorithm for global optimization. *IEEE Access*, 10, 25073-25105; <https://doi.org/10.1109/ACCESS.2022.3153493>
- Bamane, P. D. (2019, March). Application of Crow Search Algorithm to solve Real Time Optimal Power Flow Problem. In *2019 International Conference on Computation of Power, Energy, Information and Communication (ICCPEIC)* (pp. 123-129). IEEE; <https://doi.org/10.1109/ICCPEIC45300.2019.9082372>
- Birogul, S. (2019). Hybrid harris hawk optimization based on differential evolution (HHODE) algorithm for optimal power flow problem. *IEEE Access*, 7, 184468-184488; <https://doi.org/10.1109/ACCESS.2019.2958279>
- Dehghani, M., Montazeri, Z., Trojovská, E., & Trojovský, P. (2022). Coati Optimization Algorithm: A new bio-inspired metaheuristic algorithm for solving optimization problems. *Knowledge-Based Systems*, 110011; <https://doi.org/10.1016/j.knosys.2022.110011>
- Duman, S., Rivera, S., Li, J., & Wu, L. (2020). Optimal power flow of power systems with controllable wind-photovoltaic energy systems via differential evolutionary particle swarm optimization. *International Transactions on Electrical Energy Systems*, 30(4), e12270; <https://doi.org/10.1002/2050-7038.12270>
- Duong, M. Q., Nguyen, T. T., & Nguyen, T. T. (2021). Optimal placement of wind power plants in transmission power networks by applying an effectively proposed metaheuristic algorithm. *Mathematical Problems in Engineering*, 2021; <https://doi.org/10.1155/2021/1015367>
- Elattar, E. E., & ElSayed, S. K. (2019). Modified JAYA algorithm for optimal power flow incorporating renewable energy sources considering the cost, emission, power loss and voltage profile improvement. *Energy*, 178, 598-609; <https://doi.org/10.1016/j.energy.2019.04.159>
- Farhat, M., Kamel, S., Atallah, A. M., & Khan, B. (2022). Developing a Marine Predator Algorithm for Optimal Power Flow Analysis considering Uncertainty of Renewable Energy Sources. *International Transactions on Electrical Energy Systems*, 2022; <https://doi.org/10.1155/2022/3714475>
- Frank, S., & Rebennack, S. (2016). An introduction to optimal power flow: Theory, formulation, and examples. *IIE transactions*, 48, 1172-1197; <https://doi.org/10.1080/0740817X.2016.1189626>
- Frank, S., Steponavice, I., & Rebennack, S. (2012). Optimal power flow: A bibliographic survey I: Formulations and deterministic methods. *Energy systems*, 3, 221-258; <https://doi.org/10.1007/s12667-012-0056-y>
- Ginidi, A., Elattar, E., Shaheen, A., Elsayed, A., El-Sehiemy, R., & Dorrah, H. (2022). Optimal Power Flow Incorporating Thyristor-Controlled Series Capacitors Using the Gorilla Troops Algorithm. *International Transactions on Electrical Energy Systems*, 2022; <https://doi.org/10.1155/2022/9448199>
- Hassan, M. H., Kamel, S., Selim, A., Khurshaid, T., & Dominguez-Garcia, J. L. (2021). A modified Rao-2 algorithm for optimal power flow incorporating renewable energy sources. *Mathematics*, 9(13), 1532; <https://doi.org/10.3390/math9131532>
- Khunkitti, S., Siritaratiwat, A., & Premrudeepreechacharn, S. (2021). Multi-objective optimal power flow problems based on slime mould

- algorithm. *Sustainability*, 13(13), 7448; <https://doi.org/10.3390/su13137448>
- Ladumor, D. P., Trivedi, I. N., Bhesdadiya, R. H., & Jangir, P. (2017, February). Optimal Power Flow problems solution with SVC using meta-heuristic algorithm. In *2017 Third International Conference on Advances in Electrical, Electronics, Information, Communication and Bio-Informatics (AEEICB)* (pp. 283-288). IEEE; <https://doi.org/10.1109/AEEICB.2017.7972430>.
- Li, Z., Cao, Y., Dai, L. V., Yang, X., & Nguyen, T. T. (2019). Optimal power flow for transmission power networks using a novel metaheuristic algorithm. *Energies*, 12(22), 4310; <https://doi.org/10.3390/en12224310>
- Messaoudi, A., & Belkacemi, M. (2020). Optimal Power Flow Solution using Efficient Sine Cosine Optimization Algorithm. *International Journal of Intelligent Systems and Applications*, 10(2), 34; <https://www.mecs-press.org/ijisa/ijisa-v12-n2/IJISA-V12-N2-4.pdf>
- Nguyen, K. P., & Fujita, G. (2018). Self-Learning Cuckoo search algorithm for optimal power flow considering tie-line constraints in large-scale systems. *GMSARN International Journal*, 12(2), 118-126. <http://gmsarnjournal.com/home/wp-content/uploads/2018/07/vol12no2-6.pdf>
- Nguyen, T. T. (2019). A high performance social spider optimization algorithm for optimal power flow solution with single objective optimization. *Energy*, 171, 218-240; <https://doi.org/10.1016/j.energy.2019.01.021>
- Nusair, K., & Alhmod, L. (2020). Application of equilibrium optimizer algorithm for optimal power flow with high penetration of renewable energy. *Energies*, 13(22), 6066; <https://doi.org/10.3390/en13226066>
- Pandya, S. B., & Jariwala, H. R. (2020). Renewable energy resources integrated multi-objective optimal power flow using non-dominated sort grey wolf optimizer. *Journal of Green Engineering*, 10(1), 180-205; [https://journals.iau.ir/article\\_696430\\_635045319b797c9ad055404855cecf7d.pdf](https://journals.iau.ir/article_696430_635045319b797c9ad055404855cecf7d.pdf)
- Pham, L. H., Dinh, B. H., & Nguyen, T. T. (2022). Optimal power flow for an integrated wind-solar-hydro-thermal power system considering uncertainty of wind speed and solar radiation. *Neural Computing and Applications*, 1-35; <https://doi.org/10.1007/s00521-022-07000-2>
- Reddy, S.S. (2016) Optimal power flow with renewable energy resources including storage, *Electrical Engineering*, 99(2), 685–695; <https://doi.org/10.1007/s00202-016-0402-5>.
- Rojanaworahiran, K., & Chayakulkheeree, K. (2021). Probabilistic optimal power flow considering load and solar power uncertainties using particle swarm optimization. *GMSARN International Journal*, 15, 37-43; <http://gmsarnjournal.com/home/wp-content/uploads/2020/04/vol15no1-5.pdf>
- Sulaiman, M. H., & Mustafa, Z. (2021). Optimal power flow incorporating stochastic wind and solar generation by metaheuristic optimizers. *Microsystem Technologies*, 27(9), 3263-3277; <https://doi.org/10.1007/s00542-020-05046-7>
- Tiwari, S., Vaddi, N., Metta, S. B., & Kumar, M. (2020, April). Optimal power flow solution with nature inspired Antlion meta-heuristic algorithm. In *Journal of Physics: Conference Series*, 1478(1), 012035. IOP Publishing; <https://doi.org/10.1088/1742-6596/1478/1/012035>
- Tran, T. T., & Vo, N. D. (2016). Transient Stability Constrained Optimal Power Flow Using Improved Particle Swarm Optimization. *GMSARN International Journal*, 10, 87 – 94, 2016; <http://gmsarnjournal.com/home/wp-content/uploads/2016/10/vol10no3-1.pdf>.
- Warid, W. (2020). Optimal power flow using the AMTPG-Jaya algorithm. *Applied Soft Computing*, 91, 106252; <http://gmsarnjournal.com/home/wp-content/uploads/2018/07/vol12no2-6.pdf>
- Warid, W., Hizam, H., Mariun, N., Abdul-Wahab, N.I. (2016). Optimal power flow using the Jaya algorithm. *Energies*, 9(9), 678; <https://doi.org/10.3390/en9090678>
- Zimmerman, R. D., & Murillo-Sánchez, C. E. (2016). Matpower 6.0 user's manual. *Power Systems Engineering Research Center*, 9. <https://matpower.org/docs/MATPOWER-manual-6.0.pdf>



© 2023. The Author(s). This article is an open access article distributed under the terms and conditions of the Creative Commons Attribution-ShareAlike 4.0 (CC BY-SA) International License (<http://creativecommons.org/licenses/by-sa/4.0/>)